MDPI

Article

Trends of Grassland Resilience under Climate Change and Human Activities on the Mongolian Plateau

Jincheng Wu, Ziyun Sun, Ying Yao and Yanxu Liu *

State Key Laboratory of Earth Surface Processes and Resource Ecology, Faculty of Geographical Science, Beijing Normal University, Xinjiekouwai Street No. 19, Beijing 100875, China; 202011051028@mail.bnu.edu.cn (J.W.); 202011051026@mail.bnu.edu.cn (Z.S.); yaoying@mail.bnu.edu.cn (Y.Y.)
* Correspondence: yanxuliu@bnu.edu.cn

Abstract: Grassland resilience is influenced by climate change and human activities. However, little is known about how grassland resilience has changed, driven by climate change and human activities, on the Mongolian Plateau. We calculated grassland resilience on the Mongolian Plateau from 2000 to 2021 using the kernel normalized difference vegetation index (kNDVI), quantified the trends of grassland resilience using a newly proposed "critical slowing down" indicator with a machine learning algorithm, and compared the driving forces for these changes between Inner Mongolia and Mongolia. The findings of this study demonstrate that heightened levels of precipitation and reduced temperature contribute to the enhanced resilience of grassland ecosystems on the Mongolian Plateau. Conversely, the presence of grazing activities exhibits a detrimental effect on such resilience. In semi-arid regions, approximately 43% of grassland areas are undergoing a discernible decline in resilience. This decline is particularly pronounced in regions characterized by heightened levels of grazing intensity. In addition, resilience declined in 54% of areas with population growth compared with 32% in areas with population decline. Inner Mongolia, with its higher intensity of human activities, has a more serious decline in ecological resilience than Mongolia, indicating that further ecological restoration measures are needed.

Keywords: critical slowing down; temporal autocorrelation; machine learning; arid and humid conditions; grazing intensity; population density

1. Introduction

Ecological resilience refers to the capacity of ecosystems to maintain and restore their structures and functions when disturbed [1,2]. Studies have shown that climate change poses a significant threat to ecological resilience [3]. According to Levine et al., climate-change-induced stress may lead to a notable transformation of the Amazon forest into woody savannas [4]. Similarly, Zhou et al. observed significant repercussions of climate change on a subtropical, monsoon-influenced, evergreen, broad-leaved forest located in southern China [5]. Moreover, the loss of ecological resilience is more severe in regions with a greater intensity of human activities. The Amazon rainforest, for example, has been shown to lose resilience faster the closer it gets to human activity [6]. Therefore, spatiotemporal assessment of ecological resilience and identification of the driving forces can provide early warning to regions experiencing ecological degradation.

Ecological resilience can be assessed by various methods. Gazol et al. selected 775 tree-ring width chronologies from a tree-ring database, revealing the stress of extreme drought conditions on forest resilience in North America and Europe [7]. On the other hand, Xiao et al. quantified ecological resilience by employing a model that integrated aboveground and underground components, considering a set of 12 indicators [8]. Remote sensing provides all-weather, full-time, and full-coverage observations, which can also be reflected in assessing resilience [9]. Based on the Normalized Difference Water Index,

the relationship between Swiss forest resilience under the summer drought of 2018 in Central Europe and site topographic characteristics and forest stand characteristics was explored [10]. Seddon et al. developed a vegetation sensitivity index based on the enhanced vegetation index and three climate variables, including air temperature, water availability, and cloud cover, and found that vegetation resilience is sensitive to climate change [11].

In recent years, a "critical slowing down" (CSD) indicator, which includes increases in temporal autocorrelation and variance, has been proposed by ecologists as an early warning of declining ecological resilience [2,12,13]. For example, Smith et al. measured resilience using lag-one autocorrelation and variance of vegetation optical depth from 1992–2017 and found an overall decline in vegetation resilience in the equatorial rainforest belt since the early 2000s [14]. Their follow-up study added two normalized difference vegetation index (NDVI) datasets and further found that vegetation resilience declined more in regions with more pronounced interannual precipitation variability [15]. Temporal autocorrelation in the NDVI and vegetation optical depth was utilized by Verbesselt et al. to detect low resilience in tropical forests [16]. It was recently demonstrated by Forzieri et al. how global forest resilience has changed over the past 20 years through lag-one autocorrelation of the kernel normalized difference vegetation index (kNDVI) combined with machine learning methods [17]. Accordingly, remote-sensing-based "critical slowing down" indicators are increasingly being used to detect changes in vegetation resilience.

Grasslands cover 52.5 million km^2, or 40.5% of the Earth's land area excluding Greenland and Antarctica, and provide food, goods, and services to many people, including more than 1 billion low-income individuals [18–20]. Studies have shown a positive correlation between resilience and biodiversity, with grassland ecosystems typically having lower levels of resilience than forest ecosystems due to lower biodiversity [21,22]. This highlights the need for grassland resilience research. Simulations of extreme drought and midsummer heat waves were conducted in central U.S. grasslands, and it was revealed that the loss of ecosystem function due to extreme weather did not mean a decrease in resilience [23]. Hamid et al. studied the correlation between backscattering coefficients of Sentinel-1 SAR data and the NDVI in Eastern Cape, South Africa, and found that management can improve the resilience of grassland ecosystems [24]. It was also found that ponds could reduce the pressure of climate change and improve the resilience of grasslands, according to a study in Lessinia Regional Park in northern Italy [25]. Yao et al. characterized the ecological resilience of grassland to drought in China's drylands based on the area of the resilience curve fitted with drought intensity and recovery time [26]. Previous studies have characterized grassland resilience and explored its influencing factors, while little is known about the spatial trends. Moreover, the "critical slowing down" index for forests has not been tested in grasslands. Therefore, it is constructive to quantify the trend of grassland resilience and explore its drivers using the lag-one autocorrelation of the recently proposed remotely sensed vegetation index [11].

Typical temperate arid and semi-arid climates gave birth to a vast grassland belt on the Mongolian Plateau [27]. It not only supports tens of millions of local residents but also serves as an ecological barrier for hundreds of millions of people in northern China [28,29]. The Mongolian Plateau is an integral part of the ecosystem. However, because it belongs to two countries, Inner Mongolia and Mongolia, which have different ecological protection policies and inconsistent use of grasslands, it is an effective region for studying the impact of human activities on the ecosystem under global environmental change [27,30]. Studies have shown that climate change and excessive livestock grazing greatly threaten grassland resilience on the Mongolian Plateau [31–34]. This leads to the necessity of quantifying the trends of grassland resilience in the region. Taken together, our goal is to spatially identify the trends of grassland resilience on the Mongolian Plateau and reveal how climate change and human activity drive it.

2. Materials and Methods

2.1. Study Area

The Mongolian Plateau is located inland in Northeast Asia and supports the eastern part of the Eurasian steppe [35,36]. It extends through the Republic of Mongolia and the Inner Mongolia Autonomous Region of the People's Republic of China (87°45′–126°05′N, 37°24′–53°23′E) and covers an area of 2.75 million km^2 (1.17 million km^2 in Inner Mongolia and 1.58 million km^2 in Mongolia), with a population of 27.3 million persons (24 million in Inner Mongolia and 3.3 million in Mongolia).

Grasslands account for 67% of the area (Figure 1a). Grasslands on the Mongolian Plateau have high spatial variability in precipitation and temperature, with annual precipitation ranging from less than 50 mm in the central plateau to more than 400 mm in the north and east of the plateau (Figure 1b) and average temperatures ranging from nearly minus 10 °C in the northwest to more than 10 °C in the southeast (Figure 1c). Grassland distribution areas include arid and semi-arid areas (Figure 1d), with the highest nontree fractional vegetation cover in semi-arid areas (Figure 1e).
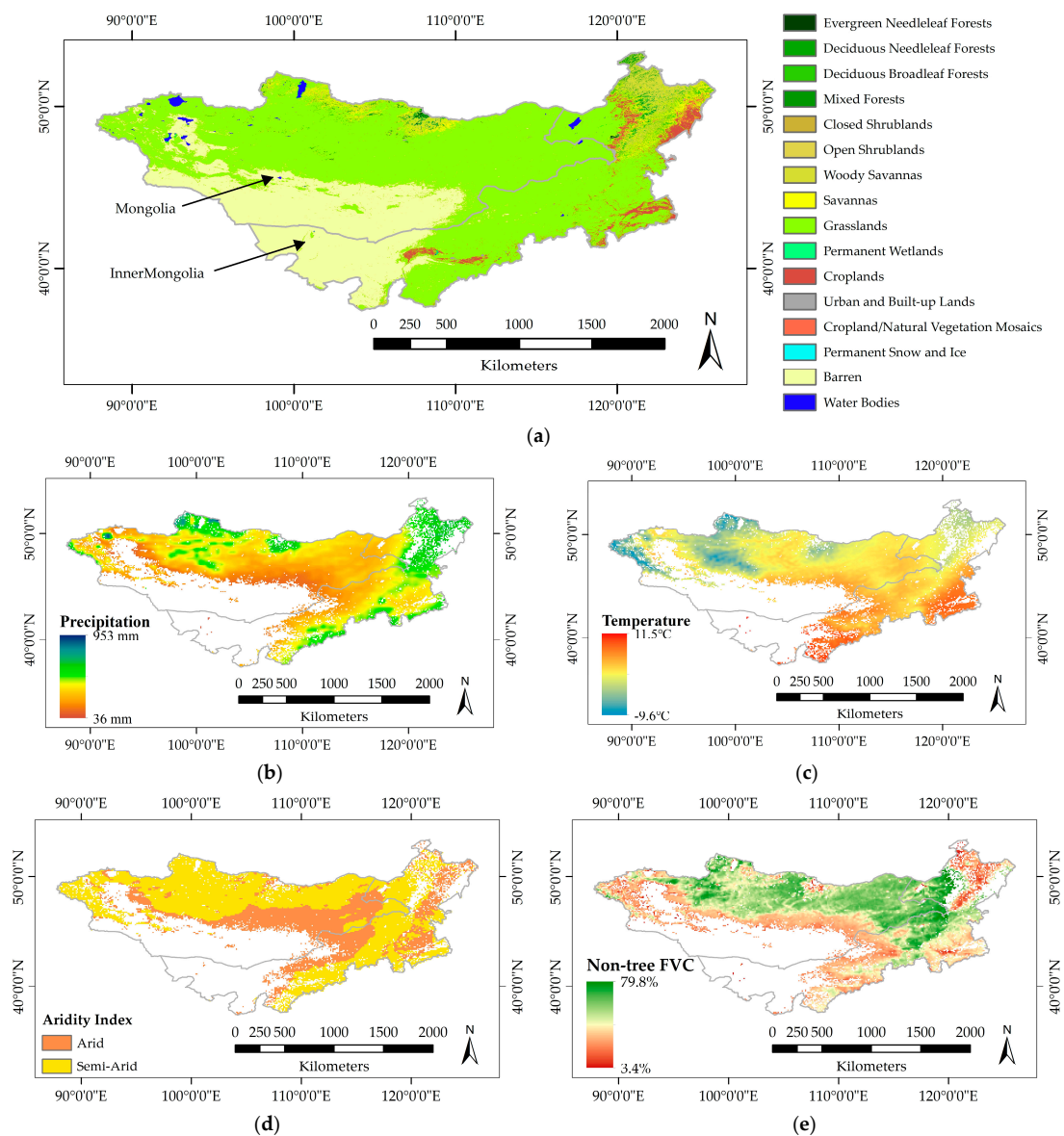
Figure 1. The geographical location and spatial patterns of (**a**) land cover types, (**b**) annual precipitation, (**c**) annual mean temperature, (**d**) aridity index, and (**e**) nontree fractional vegetation cover (FVC) of the Mongolian Plateau. White areas are the non-grassland areas.

2.2. Dataset

2.2.1. Land Cover Types

Land cover type data derived from the International Geosphere-Biosphere Programme (IGBP) at yearly intervals were acquired from the Terra and Aqua combined Moderate Resolution Imaging Spectroradiometer (MODIS) Land Cover Type (MCD12Q1) Version 6.1 data product (https://lpdaac.usgs.gov/products/mcd12q1v061/, accessed on 12 January 2023). They are extracted by masking on the Google Earth Engine (GEE) platform (https://earthengine.google.com/, accessed on 12 January 2023) using the boundary of the Mongolian Plateau. The data are at a 500 m spatial resolution, and the pixels that were grasslands both in 2001 and 2021 were defined as the range of grasslands in the study.

2.2.2. Climate Data

Climate data, including monthly averaged 2 m air temperature, surface solar radiation downwards, total evaporation, potential evaporation, and total precipitation at $0.1° × 0.1°$ horizontal resolution for 2000–2021, were acquired from the ERA5-Land reanalysis product (https://cds.climate.copernicus.eu/cdsapp#!/dataset/reanalysis-era5-land-monthly-means?tab=overview, accessed on 7 January 2023).

The aridity index was derived through the division of total precipitation by potential evaporation, as outlined in the seminal work conducted by Antonio Trabucco and Robert Zomer [37]. Based on their research findings, the resulting index values were further classified into distinct arid and semi-arid zones, employing a demarcation threshold of 0.2.

2.2.3. Vegetation Data

The nontree fractional vegetation cover (FVC) data at 250 m pixel resolution for 2000–2021 were acquired from the MOD44B Version 6 Vegetation Continuous Fields (VCF) yearly product (https://lpdaac.usgs.gov/products/mod44bv006/, accessed on 2 January 2023).

The NDVI data at a 500 m spatial resolution for 2000–2021 were acquired from the MODIS Vegetation Indices 16-Day (MOD13A1) Version 6.1 product (https://lpdaac.usgs.gov/products/mod13a1v061/, accessed on 12 Januray 2023), which was atmospherically corrected. They are monthly averaged on the GEE platform.

2.2.4. Human Activity Data

Population count grids containing estimates of the number of persons per 30-arc-second grid cell data were acquired from the Gridded Population of the World, Version 4 (GPWv4). As shown in Figure 2a, areas with high population density are mainly in Inner Mongolia. Based on data from 2000 and 2020, we divided the population growth zones, the population unchanged zones (mostly uninhabited areas), and the population reduction zones [38].
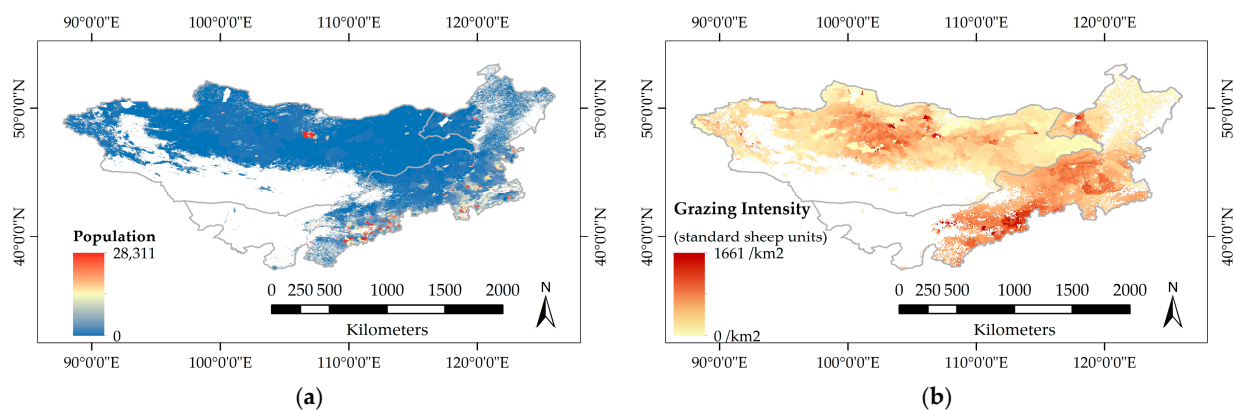
Figure 2. Distribution of (**a**) population density in 2020 (unit: number of persons per 30-arc-second grid cell); (**b**) grazing intensity (unit: standard sheep units).

Grazing intensity data were acquired from the Gridded Livestock of the World (GLW 3) database at a spatial resolution of 0.083 decimal degrees (approximately 10 km at the equator), and we selected the term dasymetric (DA) as the representation method for all species distributions [39]. Then, various types of herbivorous livestock stocking quantities were converted into standard sheep units according to the national standard, and the total grazing intensity was measured by Equation (1) as follows [40]:

$$\text{GI} = \text{N}_{\text{sheep}} + 0.9 \times \text{N}_{\text{goat}} + 5 \times \text{N}_{\text{cattle}} + 6 \times \text{N}_{\text{horses}} \tag{1}$$

in which GI is the grazing intensity, N is the number of livestock in the grid, and N's subscript refers to the corresponding livestock species. How it is distributed is shown in Figure 2b. Then, we used the upper and lower quartiles as cut-off points to classify the region into high-intensity grazing areas, medium-intensity grazing areas, and low-intensity grazing areas.

2.3. Methodology

2.3.1. Calculation of Resilience

Previous studies have proposed that vegetation resilience can be measured by the lag-one autocorrelation of the system state [14,15]. As vegetation resilience decreases, lag-one autocorrelation increases.

The kNDVI is a nonlinear generalization of the NDVI, which has been proven to improve the accuracy in monitoring some key parameters (such as gross primary productivity and leaf area index) [41]. It is therefore an ideal parameter for measuring resilience. It can be simplified by the following Equation (2):

$$\text{kNDVI} = \tan h \left(\text{NDVI}^2 \right) \tag{2}$$

The kNDVI is resampled to a resolution of $0.1° \times 0.1°$ to match the resolution of the climate data. Only pixels with NDVI values greater than zero are retained. Next, we refer to the MATLAB code developed by Giovanni Forzieri et al. to remove the seasonal trend and the long-term linear trend and obtain the kNDVI anomalies [42]. Then, we calculate the lag-one autocorrelation for the whole kNDVI anomaly time series (2000–2021) using Equation (3) and call it the long-term temporal autocorrelation (TAC). The lag-one TAC can be calculated by Equation (3) as follows:

$$\text{lag-one TAC} = \frac{(y_2 - \overline{y})(y_1 - \overline{y}) + (y_3 - \overline{y})(y_2 - \overline{y}) + \cdots + (y_n - \overline{y})(y_{n-1} - \overline{y})}{(y_1 - \overline{y})^2 + (y_2 - \overline{y})^2 + \cdots + (y_n - \overline{y})^2} \tag{3}$$

in which y is the time-series data, the subscript to y represents its serial number, and $\overline{y}$ refers to the mean value of data y.

2.3.2. Resilience Driver Analysis and Trend Calculation

We applied a random forest (RF) regression model to explore the environmental drivers of the long-term TAC. Referring to the study by Forzieri et al., we selected four categories of drivers, including vegetation attributes, climate background, climate variability, and climate autocorrelation [17]. For vegetation attribute drivers, we considered nontree fractional vegetation cover. For climate drivers, we considered 2 m air temperature, surface solar radiation downwards, total precipitation, and evapotranspiration deficit (calculated by subtracting total evapotranspiration from total precipitation). All variables, except those belonging to climate autocorrelation, which are calculated similarly to long-term TAC, were first calculated on an annual basis and then on a multiyear average. All variables are shown in Table 1.

Table 1. Variables used in the random forest regression model.

Variable Name [1]	Category	Label
Average Nontree Fractional Vegetation Cover	Vegetation Attributes	FVC.VA
Growing-season-averaged kNDVI	Vegetation Attributes	GSkNDVI.VA
Average 2 m Air Temperature	Climate Background	TEMP.CB
Variable Coefficient of 2 m Air Temperature	Climate Variability	TEMP.CV
Temporal Autocorrelation of 2 m Air Temperature	Climate Autocorrelation	TEMP.CA
Average Surface Solar Radiation Downwards	Climate Background	SSRD.CB
Variable Coefficient of Surface Solar Radiation Downwards	Climate Variability	SSRD.CV
Temporal Autocorrelation of Surface Solar Radiation Downwards	Climate Autocorrelation	SSRD.CA
Average Total Precipitation	Climate Background	PRCP.CB
Variable Coefficient of Total Precipitation	Climate Variability	PRCP.CV
Temporal Autocorrelation of Total Precipitation	Climate Autocorrelation	PRCP.CA
Average Evapotranspiration Deficit	Climate Background	ETD.CB
Variable Coefficient of Evapotranspiration Deficit	Climate Variability	ETD.CV
Temporal Autocorrelation of Evapotranspiration Deficit	Climate Autocorrelation	ETD.CA

[1] All the variables were selected by referring to the study by Forzieri et al. [17]. In all ecosystems, the most important climate factors are temperature, precipitation, evapotranspiration, and radiation. Previous studies of grasslands have also paid attention to temperature, precipitation, evapotranspiration, and radiation [43,44].

During RF model development, we sampled all pixels and divided all the samples into two datasets: 60% for the training set and 40% for the testing set. We used 100 regression trees with a leaf size of 1.

Then, we used the RF regression model to explore the trends of grassland resilience over the past 2 decades. We calculated the temporal autocorrelation of the kNDVI anomalies over a 3-year moving window to obtain the time series TAC^t. We then input all annual environmental drivers into the RF regression model to calculate TAC_1^t and control the climate autocorrelation variables for the first-year value to calculate TAC_2^t. TAC_{ac}^t is obtained from $TAC_1^t - TAC_2^t$, which is the part of TAC^t that changes over time due to climate autocorrelation. We isolated TAC_{ac}^t from TAC^t and obtained the enhanced TAC. The linear trend of enhanced TAC, which shows the trend of grassland resilience change, is called δTAC. Then, we isolated the impact of human activities by observing how grassland resilience is distributed in areas with different population change trends and grazing intensities. Finally, we investigated the environmental drivers of the long-term TAC by developing a new RF regression model similar to the previous one.

A flow chart is presented in Figure 3.
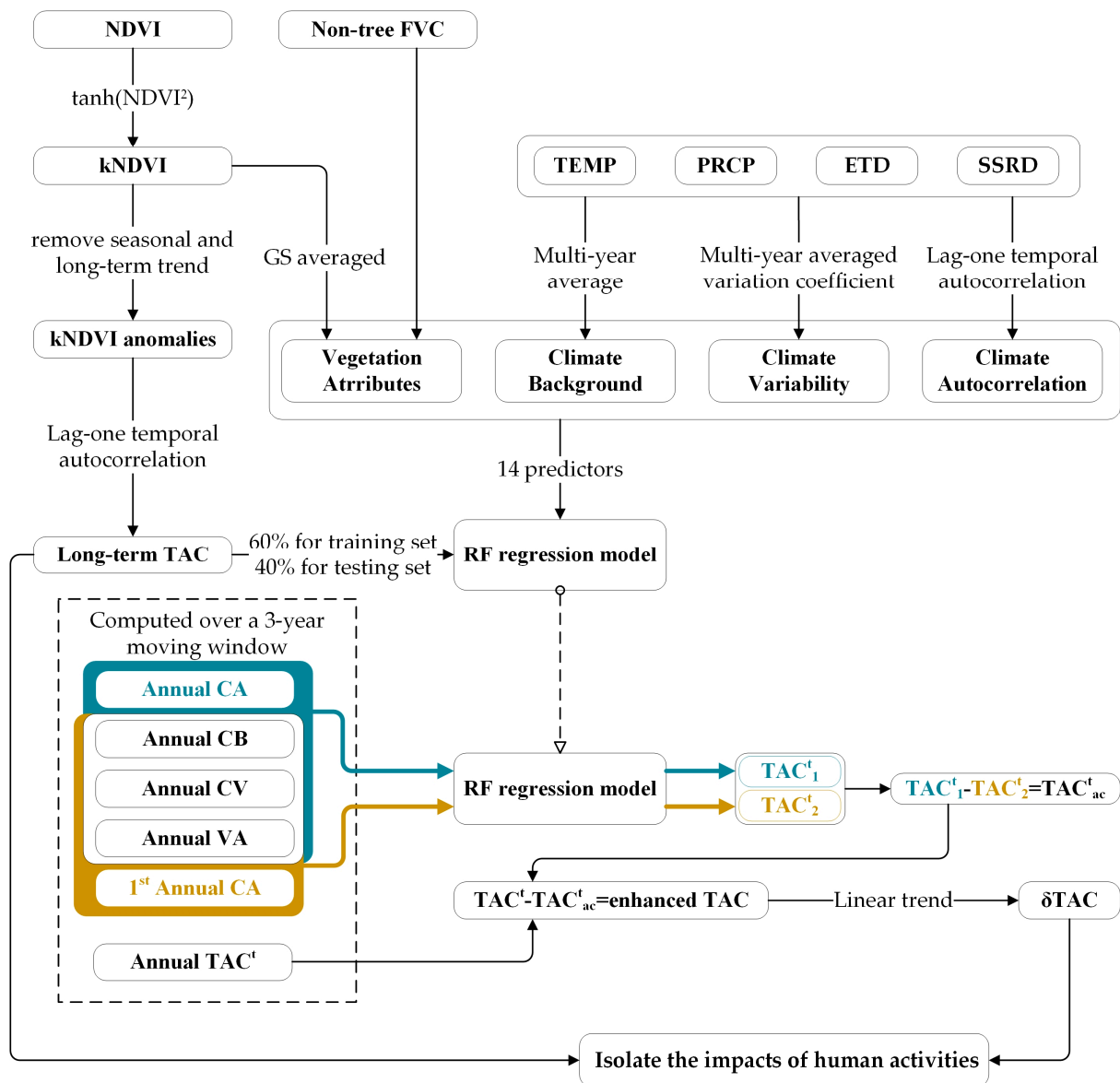
Figure 3. Technical flow chart for the data analysis. CA, CB, CV, and VA refer to all variables that belong to Climate Autocorrelation, Climate Background, Climate Variability, and Vegetation Attributes, respectively.

3. Results

3.1. Grassland Resilience of the Mongolian Plateau and Its Key Drivers

The average nontree fractional vegetation cover in the grasslands of the Mongolian Plateau year by year in Figure 4 shows an overall fluctuating decline in nontree fractional vegetation cover, from 56% in 2000 to 52% in 2021, reaching a maximum of 57% in 2010 and a minimum of 47% in 2018. The decline in grassland fractional vegetation cover is an early warning of vegetation degradation on the Mongolian Plateau.

The greater the long-term TAC, the worse the grassland resilience. Figure 5a shows the spatial distribution of the long-term TAC. In the north and the northeast, the grassland has better resilience. Figure 5b shows changes in the long-term TAC under different temperature and precipitation conditions. The results show that the grassland has good resilience in areas with high annual precipitation and low temperature in the range of precipitation and temperature in the study area. Figure 5c shows that the long-term TAC values in areas with medium or high grazing intensity are higher than those in the whole grassland. This means that grazing intensity is negatively associated with grassland

resilience, which is worse in areas with higher grazing intensity. Similarly, Figure 5d shows that resilience in semi-arid areas is better than that in arid areas.
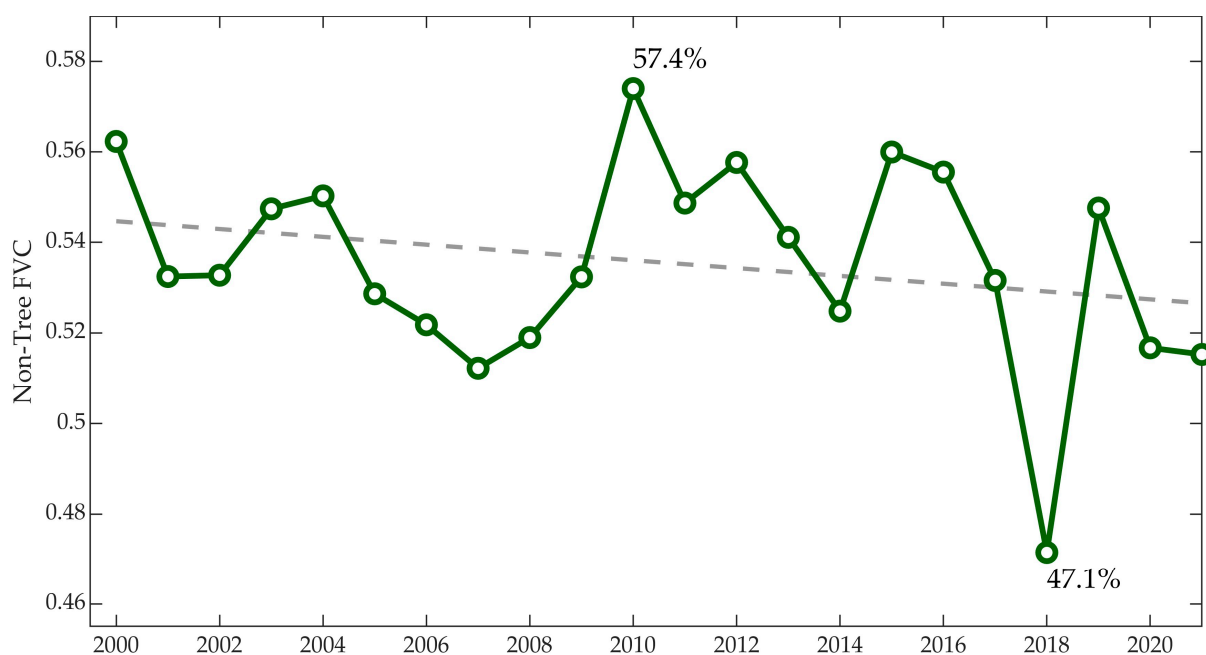
Figure 4. Time series of average nontree fractional vegetation cover in grasslands of the Mongolian Plateau. The numbers show the maximum and the minimum of the time series, while the gray line shows its linear trend.

Considering the temporal differences in resilience, Figure 5e shows how grassland resilience has changed over the last decade (2011–2021) compared to the previous decade (2000–2010). We found that 41% of grasslands across the Mongolian Plateau experienced a loss of resilience in the last decade. In semi-arid areas, up to 44% of grasslands have experienced a loss of resilience in the last decade, compared to only 36% in arid areas. This indicates that the most serious loss of grassland resilience on the Mongolian Plateau is in wetter areas. Correspondingly, grasslands with higher resilience lose more of their resilience.

As shown in Figure 6a, the model explains 91.2% of the spatial variance of the long-term TAC (R^2) with a mean squared error (MSE) of 0.043. The rank of the corresponding variable importance of the independent variable on long-term TAC is shown in Figure 6b. The four variables with greater corresponding variable importance are the variable coefficient of surface solar radiation downwards, temporal autocorrelation of surface solar radiation downwards, variable coefficient of total precipitation, and growing-season-averaged kNDVI, followed by the variables averaged 2 m air temperature and total precipitation. The evapotranspiration deficit variables are the least important.

Furthermore, we also explore the response of the long-term TAC to every single variable when others are unchanged by using partial dependence plots (Figure 6c). FVC.VA promotes long-term TAC. GSkNDVI.VA reduces the long-term TAC due to higher resilience in areas with high vegetation. Moisture conditions contribute to the resilience of vegetation, so the long-term TAC decreases with the increases in PRCP.CB but has little effect on long-term TAC when precipitation decreases or increases to a certain extent. The effect of SSRD.CB on the long-term TAC is stepwise promoted, with an increase in long-term TAC and a decrease in resilience with SSRD.CB. Long-term TACs respond to TEMP.CB in a nonmonotonous manner. The cooler or higher the temperature is, the lower the long-term TAC, meaning that both high and low temperatures increase vegetation resilience. ETD.CB affects resilience, and we note that when evaporation is greater than precipitation, the larger ETD.CB is, the smaller the long-term TAC; when evaporation is smaller than precipitation, ETD.CB has little effect on long-term TAC. In addition, PRCP.CV, SSRD.AC, and ETD.CV

have less impact on resilience, with a slight increase in long-term TAC as PRCP.CV and SSRD.AC increase. Overall, increases in TEMP.CV and PRCP.AC lead to an increase in long-term TAC. An increase in SSRD.CV, TEMP.AC, and ETD.AC leads to a decrease in long-term TAC, but an increase in SSRD.CV to 0.5 leads to an increase in long-term TAC.
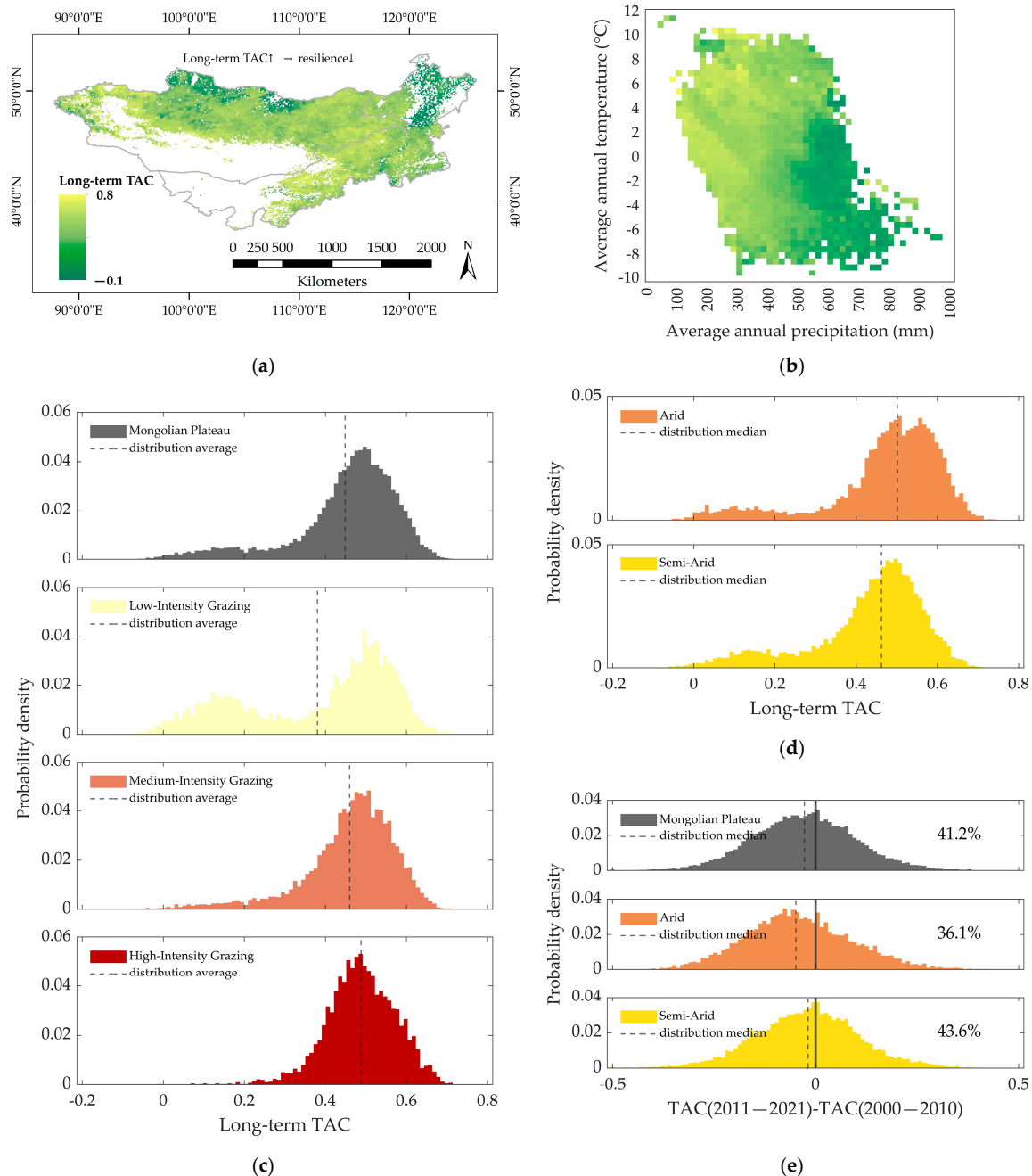
Figure 5. Spatial and temporal variations in the long-term TAC on the Mongolian Plateau and some important drivers. (**a**) A spatial map of the long-term TAC. White areas are the non-grassland areas or no-data areas. (**b**) The mean value of long-term TAC under different temperature and precipitation gradients. (**c**) Frequency distribution of the long-term TAC under different grazing intensities and (**d**) wetness conditions. The dashed line in each subgraph shows the distribution average. (**e**) Frequency distribution of the difference in the long-term TAC between the two decades under different wetness conditions. The thick line in each subgraph shows zero, while the dashed line shows the distribution median. The number in each subgraph indicates the percentage of the samples that are greater than zero.

(**a**)

(**b**)

(**c**)
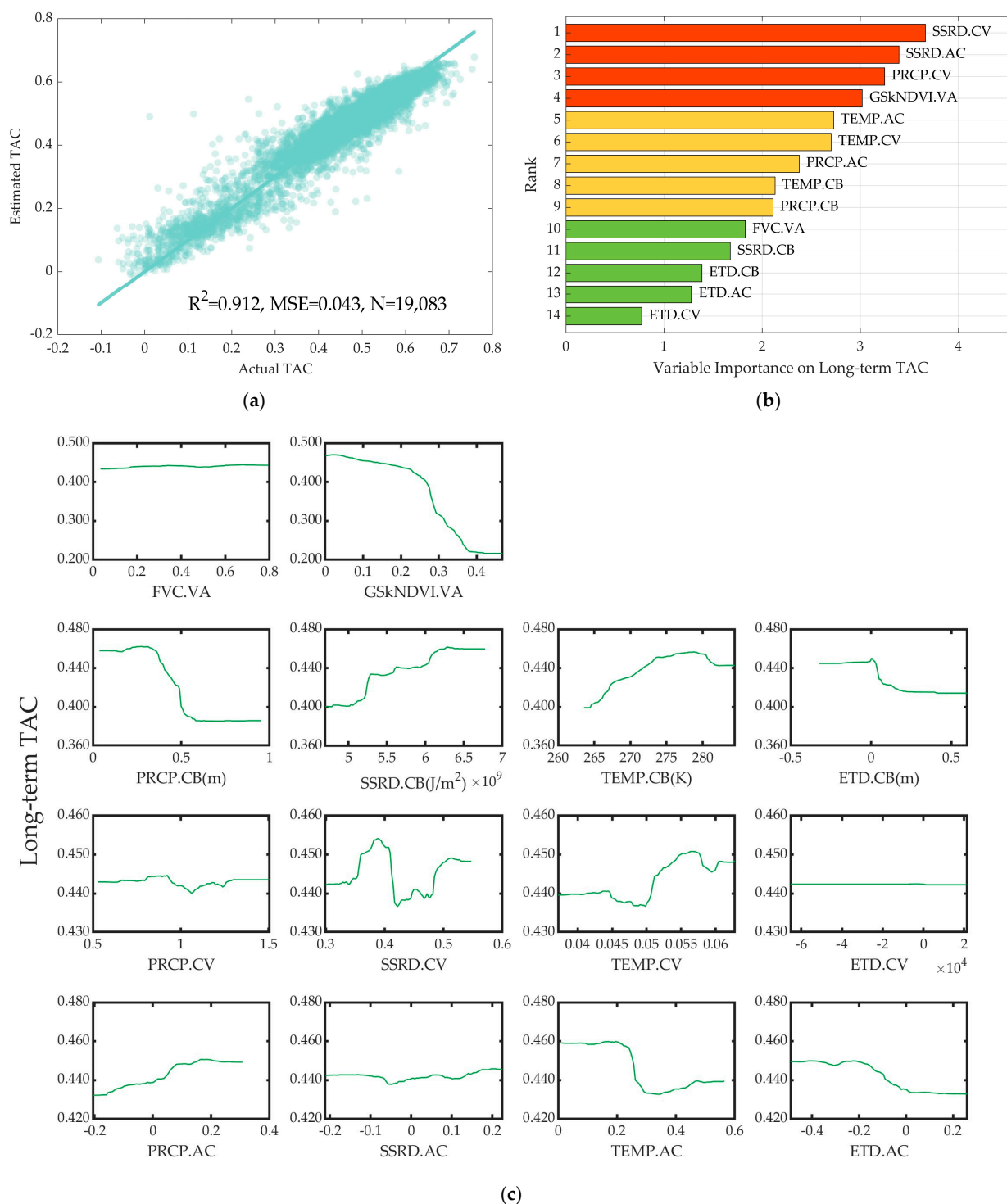
Figure 6. The results of the random forest regression model developed to investigate the environmental drivers of long-term TAC. (**a**) Scatter plot of the actual long-term TAC and estimated long-term TAC. N means the number of samples. (**b**) Corresponding variable importance of the independent variable on long-term TAC. (**c**) Partial dependence plot of the long-term TAC with each dependent variable based on the random forest regression model, reflecting the response of the long-term TAC to a single variable when others are unchanged.

3.2. Trend of Grassland Resilience on the Mongolian Plateau and Its Key Drivers

According to Figure 7a, the loss of grassland resilience is the most serious in the eastern and northeastern parts of the Mongolian Plateau. Figure 7b shows the average δTAC at

different temperatures and precipitation conditions, indicating that grassland resilience is improved in areas with higher temperatures, while in areas with higher precipitation, grassland resilience is lost. Figure 7c shows that the wetter the area is, the greater the loss of resilience. It also shows that wetter areas are more resilient, consistent with the pattern shown in Figure 5d. Figure 7d shows the decline in resilience in areas with higher grazing intensity. In high-intensity grazing areas, 57% of grassland areas suffered a loss of resilience, compared to 40% and 44% in low-intensity and medium-intensity areas, respectively. Figure 7e shows the impact of population change on grassland resilience. In areas of population growth, 54% of grassland areas experience a loss of resilience, compared with 45% and 32% in areas of constant population and population decline, respectively. Population changes can partly reflect changes in the intensity of human activity, and this finding reveals a relative consistency between trends in population changes and trends in resilience.
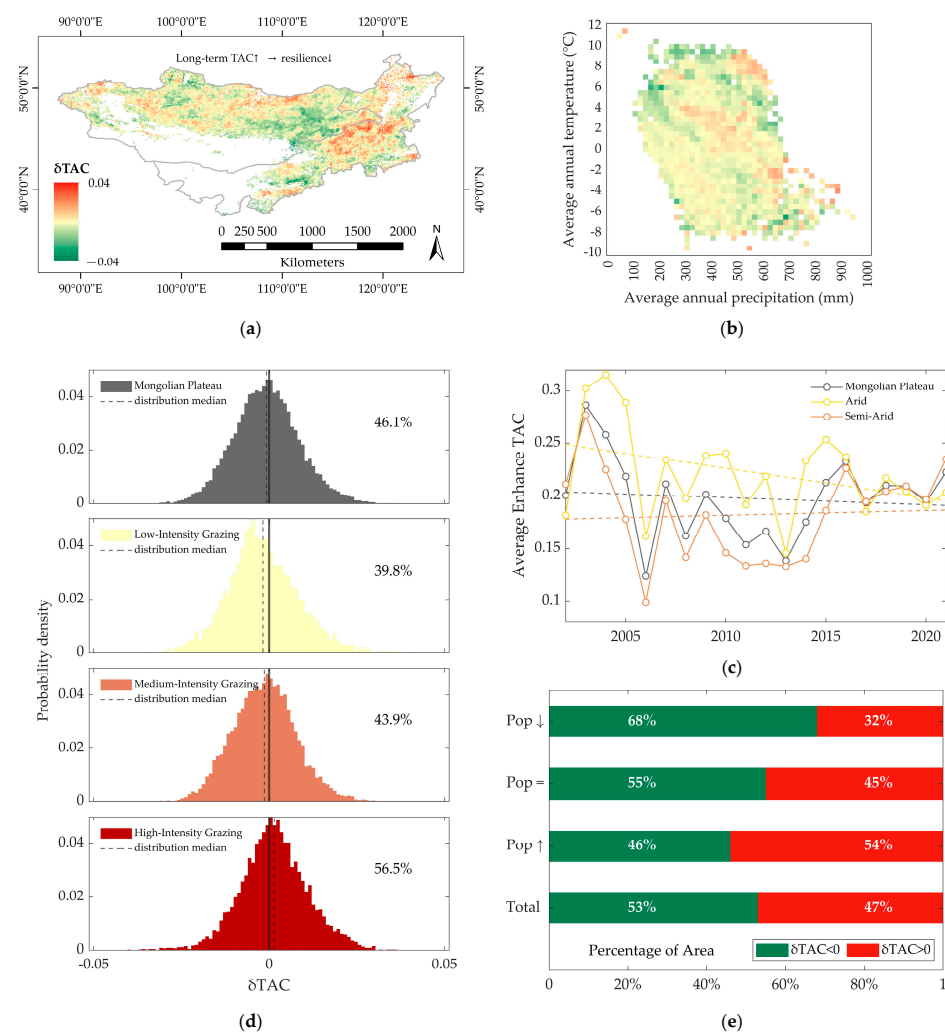
Figure 7. Spatial variations in the trend of enhanced TAC on the Mongolian Plateau and some important drivers. (**a**) A spatial map of the δTAC. (**b**) The mean value of δTAC under different temperature and precipitation gradients. (**c**) Temporal changes in enhanced TAC separately for the Mongolian Plateau, the arid region, the semi-arid region, and the dry subhumid and humid region. The dotted lines are the fitting lines. (**d**) Frequency distribution of the δTAC under different grazing intensities. The thick line in each subgraph shows zero, while the dashed line shows the distribution median. The number in each subgraph indicates the percentage of the samples that are greater than zero. (**e**) Percentage of the area where δTAC is greater than 0 or less than 0 under different population change conditions.

The new RF model explains 76.4% of the spatial variation in δTAC (R^2) with a mean square error (MSE) of 0.0046 (Figure 8a). Among the environmental variables, those relating to surface solar radiation downwards, total precipitation, and 2 m air temperature remain important, but those about vegetation properties (growing-season-averaged kNDVI and fractional vegetation cover) are less important, and those about evapotranspiration deficit remain the least important factors (Figure 8b).
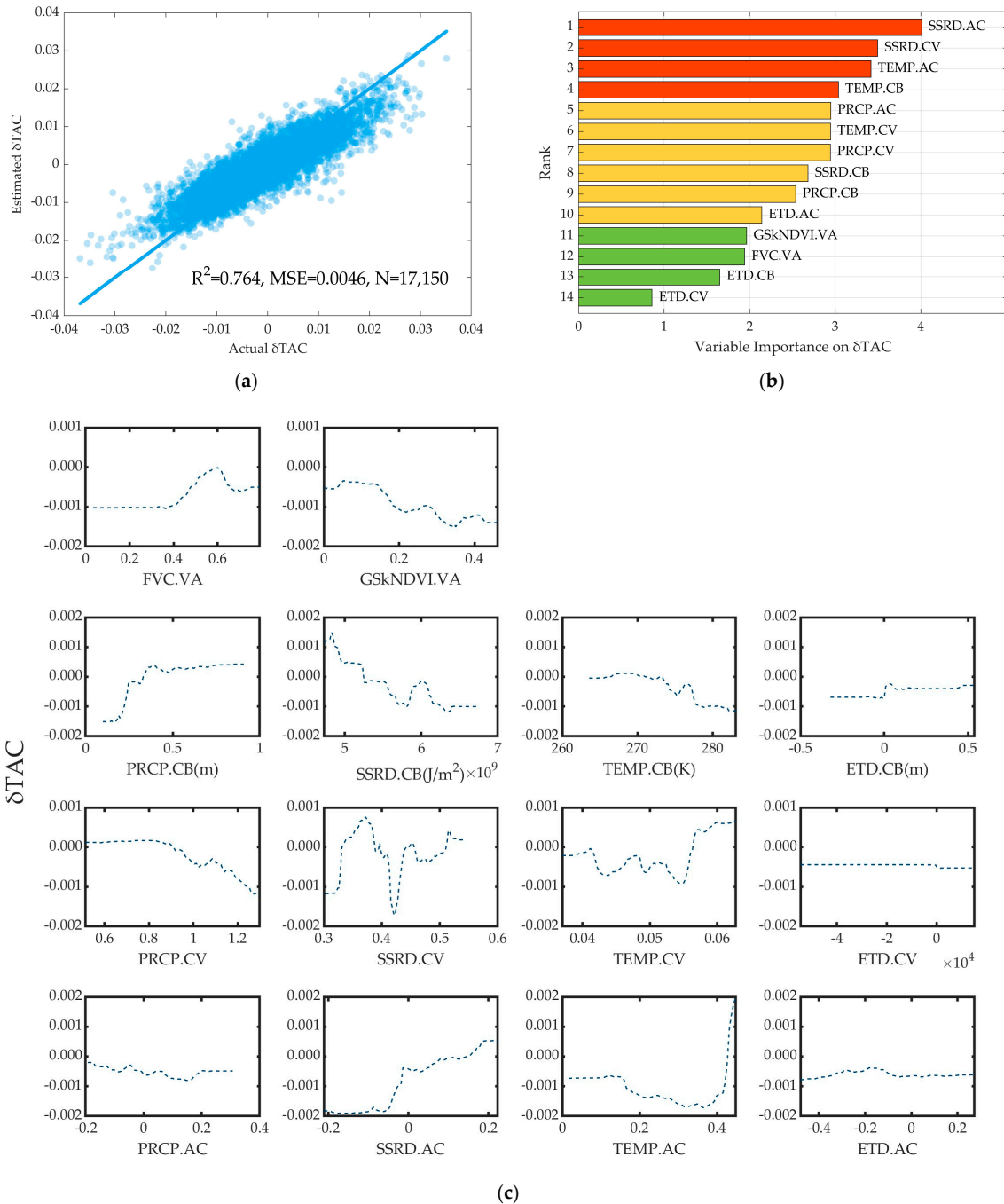
Figure 8. The results of the random forest regression model developed to investigate the environmental drivers of δTAC. (**a**) Scatterplot of actual δTAC and estimated δTAC. N means the number of samples. (**b**) Corresponding variable importance of the independent variable on δTAC. (**c**) Partial dependence plot of the δTAC with each dependent variable based on the random forest regression model, reflecting the response of the δTAC to a single variable when others are unchanged.

The responses of δTAC to a single variable are shown in Figure 8c. δTAC is non-monotonous in response to FVC and is smaller in areas where FVC is higher or lower. Vegetation greenness has a positive effect on the trend of resilience change, with GSkNDVI increasing and δTAC decreasing. Resilience loss tends to be more severe in areas with higher precipitation and evapotranspiration deficits, with δTAC increasing with the increase in PRCP.CB. Both solar radiation and temperature are positive for trends of resilience changes, with δTAC fluctuations decreasing with SSRD.CB or TEMP.CB. δTAC decreases with increasing PRCP.CV. The response of δTAC to SSRD.CV and TEMP.CV is more complex, and with the increase in SSRD.CV and TEMP.CV, δTAC shows an overall oscillatory upward trend. δTAC increases with SSRD.AC, while its response to the autocorrelation of precipitation, temperature, and evapotranspiration deficits is nonmonotonous, with δTAC being larger at higher and lower levels of either PRCP.AC or TEMP.AC and smaller where ETD.AC is higher and lower. In addition, ETD.CV has little impact on resilience trends, with a slight decrease in δTAC as ETD.CV increases.

4. Discussion

4.1. Comparison of Grassland Resilience and Its Trend between Inner Mongolia and Mongolia

The Mongolian Plateau belongs to two different countries that have inconsistent uses of grassland. In addition to grazing, the primary disturbance factor affecting grassland ecosystems in Inner Mongolia is attributed to industrial activities, while in Mongolia, the main source of disruption arises from reclamation [27].

When considering grazing intensity and population density, the disparity in human activities between Inner Mongolia and Mongolia becomes more evident. This contrast is visually depicted in Figure 9a,b, where it can be observed that a greater proportion of areas in Inner Mongolia exhibit high-intensity grazing (46% compared to 12% in Mongolia) and obvious population growth (50% compared to 6% in Mongolia).
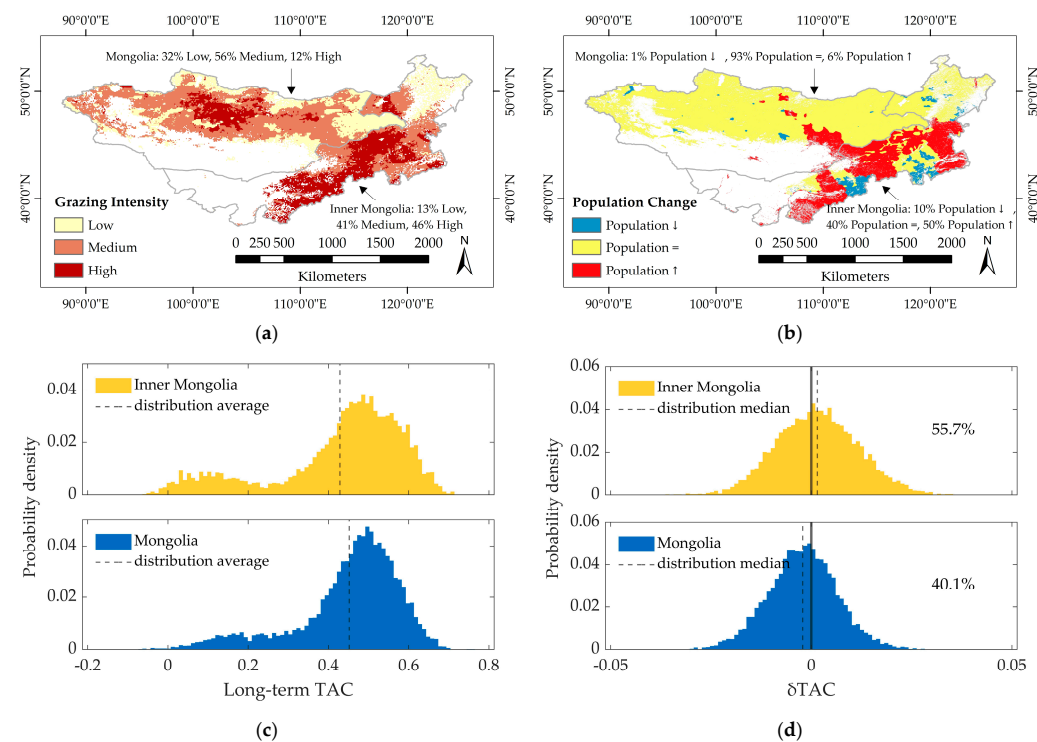
Figure 9. Comparison of (**a**) grazing intensity, (**b**) population change, (**c**) long-term TAC, and (**d**) δTAC in Inner Mongolia and Mongolia. The thick line in each subgraph in (**c**,**d**) shows zero, while the dashed line shows the distribution average in (**c**) and the distribution median in (**d**). The number in each subgraph in (**d**) indicates the percentage of the samples that are greater than zero.

As shown in Figure 9c, Inner Mongolia is slightly more resilient than Mongolia, with more distribution in the low-value regions of long-term TAC. The main reason may be that Inner Mongolia has a wetter climate than Mongolia. However, in terms of trends, 56% of grasslands in Inner Mongolia experienced resilience loss, compared to 40% in Mongolia (Figure 9d). Although the reasons for the variation in vegetation resilience between Inner Mongolia and Mongolia are complex, the difference in the intensity of human activities can be an influential factor. Inner Mongolia has 11 times the population density of Mongolia (23.3 persons per km^2 in Inner Mongolia and 2.1 persons per km^2 in Mongolia). The average grazing intensity is 49.5 units of sheep per km^2 in Inner Mongolia and 25.1 units of sheep per km^2 in Mongolia. Considering that the average precipitation in Inner Mongolia is even somewhat higher than that in Mongolia (406 mm average annual precipitation in Inner Mongolia and 328 mm in Mongolia), the impacts of differences in the intensity of human activities are pronounced.

When we control for similar population change or grazing intensity, as shown in Table 2, the differences between Inner Mongolia and Mongolia are smaller under high-intensity grazing conditions, whereas this does not occur in areas with population growth. This further shows that the difference in grazing intensity is an important reason for the difference in the trends of grassland resilience in Inner Mongolia and Mongolia. Although some previous studies have noted that the effects of climate change are dominant factors [30,34], our findings support that grazing intensity is a key factor in grassland degradation on the Mongolian Plateau, which is consistent with the work of Liang et al. [45]. Our study directly compares the distribution of grassland resilience under different grazing intensities, which was not available in previous studies.

Table 2. Average and variable coefficients of δTAC in Inner Mongolia and Mongolia under the same control of grazing intensity/population change.

	Inner Mongolia		Mongolia		Mongolian Plateau	
	Mean	**CV [1]**	**Mean**	**CV**	**Mean**	**CV**
Whole	0.0015	6.7743	−0.0021	−3.9831	−0.0007	−12.8030
Low-Intensity	0.0035	2.8290	−0.0028	−3.3634	−0.0017	−5.6944
Medium-Intensity	0.0004	23.1531	−0.0022	−3.7341	−0.0014	−6.4395
High-Intensity	0.0022	4.7340	−0.0002	−29.7911	0.0015	6.4951
Population ↑ [2]	0.0026	4.2351	−0.0083	−1.0288	0.0009	12.0709
Population =	0.0020	4.4488	−0.0017	−4.8079	−0.0009	−9.2848
Population ↓	−0.0038	−2.4678	−0.0001	−167.7656	−0.0032	−3.0504

[1] CV stands for the variable coefficient. [2] The symbols "↑", "=", and "↓" stand for the population growth, costant population, and population decline, respectively.

Taken together, our study provides monitoring for the trend of ecological resilience loss on the Mongolian Plateau, especially in Inner Mongolia, which suffers more than Mongolia due to differences in drivers such as grazing intensity. The Mongolian Plateau as a whole needs more ecological restoration projects, especially in Inner Mongolia.

4.2. The Spatial Distribution and Drivers of Grassland Resilience and Its Trend on the Mongolian Plateau

We found that grassland resilience is higher in the northern and northeastern Mongolian Plateau, where the surrounding ecosystems are more complex with greater biodiversity. This finding is consistent with the previous study by Oliver et al., which considered that biodiversity is crucial for ecological resilience [22]. It is found that grassland resilience is better with higher precipitation and lower temperature on the Mongolian Plateau, which is consistent with the study by Gibson et al. [46]. According to Verhoeve et al., the reason why higher temperatures lead to lower resilience may be that higher temperatures lead to higher potential evaporation rates, which exacerbates drought [47].

For trends of resilience, in Inner Mongolia, the decline in resilience was mainly in the central and eastern regions, while in Mongolia, it was mainly in the northwest and north. We observed that in Inner Mongolia, the spatial distribution of areas with declined resilience overlapped somewhat with areas with declining populations, whereas in Mongolia, areas with declined resilience overlapped more spatially with areas with high-intensity grazing. Moreover, vegetation resilience in arid regions is improving, which is consistent with the study on forest resilience by Gazol et al. [7].

In new findings, we found that on the Mongolian Plateau, climate variability has a greater influence than climate mean, which is not consistent with the findings of the study on the global scale by Feng et al. [3]. The conclusion in the study on the global scale is not necessarily true in the region and may even be quite the opposite, further confirming the need for a regional-scale study of regional problems. Therefore, the law obtained from the study of grassland resilience on the Mongolian Plateau is more effective in guiding the ecological restoration measures in this area than the law of global universality. Moreover, previous studies have paid little attention to the effects of radiation on resilience, and we observed the importance of radiation to both resilience and resilience trends on the Mongolian Plateau.

4.3. Uncertainty of Method and Potential Future Improvement

In our study, climate data are for 2000–2021, while the livestock data are for 2010, but it is already the most recent available dataset. Moreover, the livestock data are a global-scale dataset, and uncertainties may exist at the regional scale. However, it has performed well in many previous regional-scale studies, for example, Hankerson et al.'s study in Kazakhstan and Bond et al.'s study in Africa [48,49].

The study considers 14 predictors when developing an RF regression model. However, it is unclear what impact other unconsidered climate factors may have on the quantification of resilience.

Moreover, population changes might not accurately reflect the changes in the intensity of human activities. Changes in the intensity of human activity are also associated with changes in productive lifestyles.

Furthermore, when analyzing the impact of human activities on resilience, different conditions are not quantified by their relative weight. In further studies, it may be improved by developing models to quantify the contribution of human activities (e.g., grazing) to the distribution patterns and trends of resilience.

5. Conclusions

The purpose of our study is to explore the spatial distribution pattern, change trend, and driving factors of grassland resilience on the Mongolian Plateau. Five main findings are concluded as follows. First, the distribution of grassland resilience on the Mongolian Plateau is constrained by precipitation and temperature. Grasslands are less resilient in areas with high precipitation and low temperatures, but they are becoming more resilient in areas with high temperatures. Second, grasslands in semi-arid areas show a more serious decline in resilience, with 44% of the area experiencing a decline in resilience, compared with 36% and 41% in arid regions and the Mongolian Plateau as a whole. Third, grazing intensity has a negative impact on grassland resilience and its trend. In areas with high grazing intensity, grassland resilience is lower, and the decline is more noticeable. A total of 57% of grasslands in high-intensity grazing areas experienced a loss of resilience, compared to 40%, 44%, and 46% in low-intensity grazing areas, medium-intensity grazing areas, and the Mongolian Plateau as a whole, respectively. Fourth, the trend of population change is relatively consistent with the trend of grassland resilience on the Mongolian Plateau. A total of 54% of grasslands in areas of population growth experience resilience loss, compared to 32%, 45%, and 47% in declining areas, unchanged areas, and the Mongolian Plateau as a whole, respectively. Finally, Inner Mongolia is slightly more ecologically resilient than Mongolia, possibly due to climatic conditions such as precipitation and radiation. However,

Inner Mongolia's ecological resilience has declined significantly more than that of Mongolia over the past 20 years. In Inner Mongolia, 56% of grasslands suffer a loss of resilience, compared to 40% in Mongolia. The main driving factor of the variation in the resilience trend is the difference in grazing intensity between Inner Mongolia and Mongolia.

We developed the application of the "critical slowing down" indicator in the calculation of grassland resilience, which has been used mostly in forest ecosystems in previous studies. In our research, we used it to spatially identify grassland resilience and its trends on the Mongolian plateau. We found that solar radiation plays an important role in grassland resilience, which has not been observed in previous studies. The role of solar radiation could be covered more in future studies of grassland resilience. Our findings suggest that ecological restoration is still needed on the Mongolian Plateau, especially in Inner Mongolia, to reverse the declining trend of grassland resilience on the Mongolian Plateau, especially in Inner Mongolia.

Conflicts of Interest: The authors declare no conflict of interest.

References

1. Folke, C.; Carpenter, S.; Walker, B.; Scheffer, M.; Elmqvist, T.; Gunderson, L.; Holling, C.S. Regime Shifts, Resilience, and Biodiversity in Ecosystem Management. *Annu. Rev. Ecol. Evol. Syst.* **2004**, *35*, 557–581. [CrossRef]
2. Scheffer, M.; Carpenter, S.R.; Dakos, V.; van Nes, E.H. Generic Indicators of Ecological Resilience: Inferring the Chance of a Critical Transition. *Annu. Rev. Ecol. Evol. Syst.* **2015**, *46*, 145–167. [CrossRef]
3. Feng, Y.; Su, H.; Tang, Z.; Wang, S.; Zhao, X.; Zhang, H.; Ji, C.; Zhu, J.; Xie, P.; Fang, J. Reduced resilience of terrestrial ecosystems locally is not reflected on a global scale. *Commun. Earth Environ.* **2021**, *2*, 88. [CrossRef]
4. Levine, N.M.; Zhang, K.; Longo, M.; Baccini, A.; Phillips, O.L.; Lewis, S.L.; Alvarez-Dávila, E.; Segalin de Andrade, A.C.; Brienen, R.J.W.; Erwin, T.L.; et al. Ecosystem heterogeneity determines the ecological resilience of the Amazon to climate change. *Proc. Natl. Acad. Sci. USA* **2016**, *113*, 793–797. [CrossRef]
5. Zhou, G.; Peng, C.; Li, Y.; Liu, S.; Zhang, Q.; Tang, X.; Liu, J.; Yan, J.; Zhang, D.; Chu, G. A climate change-induced threat to the ecological resilience of a subtropical monsoon evergreen broad-leaved forest in Southern China. *Glob. Chang. Biol.* **2013**, *19*, 1197–1210. [CrossRef] [PubMed]

6.   Boulton, C.A.; Lenton, T.M.; Boers, N. Pronounced loss of Amazon rainforest resilience since the early 2000s. *Nat. Clim. Chang.* **2022**, *12*, 271–278. [CrossRef]

7.   Gazol, A.; Camarero, J.J.; Anderegg, W.R.L.; Vicente-Serrano, S.M. Impacts of droughts on the growth resilience of Northern Hemisphere forests. *Glob. Ecol. Biogeogr.* **2017**, *26*, 166–176. [CrossRef]

8.   Xiao, W.; Lv, X.; Zhao, Y.; Sun, H.; Li, J. Ecological resilience assessment of an arid coal mining area using index of entropy and linear weighted analysis: A case study of Shendong Coalfield, China. *Ecol. Indic.* **2020**, *109*, 105843. [CrossRef]

9.   Pei, T.; Xu, J.; Liu, Y.; Huang, X.; Zhang, L.; Dong, W.; Qin, C.; Song, C.; Gong, J.; Zhou, C. GIScience and remote sensing in natural resource and environmental research: Status quo and future perspectives. *Geogr. Sustain.* **2021**, *2*, 207–215. [CrossRef]

10. Sturm, J.; Santos, M.J.; Schmid, B.; Damm, A. Satellite data reveal differential responses of Swiss forests to unprecedented 2018 drought. *Glob. Chang. Biol.* **2022**, *28*, 2956–2978. [CrossRef]

11. Seddon, A.W.R.; Macias-Fauria, M.; Long, P.R.; Benz, D.; Willis, K.J. Sensitivity of global terrestrial ecosystems to climate variability. *Nature* **2016**, *531*, 229–232. [CrossRef]

12. Dakos, V.; Carpenter, S.R.; van Nes, E.H.; Scheffer, M. Resilience indicators: Prospects and limitations for early warnings of regime shifts. *Philos. Trans. R. Soc. B Biol. Sci.* **2015**, *370*, 20130263. [CrossRef]

13. Scheffer, M.; Bascompte, J.; Brock, W.A.; Brovkin, V.; Carpenter, S.R.; Dakos, V.; Held, H.; van Nes, E.H.; Rietkerk, M.; Sugihara, G. Early-warning signals for critical transitions. *Nature* **2009**, *461*, 53–59. [CrossRef]

14. Smith, T.; Traxl, D.; Boers, N. Empirical evidence for recent global shifts in vegetation resilience. *Nat. Clim. Chang.* **2022**, *12*, 477–484. [CrossRef]

15. Smith, T.; Boers, N. Global vegetation resilience linked to water availability and variability. *Nat. Commun.* **2023**, *14*, 498. [CrossRef] [PubMed]

16. Verbesselt, J.; Umlauf, N.; Hirota, M.; Holmgren, M.; Van Nes, E.H.; Herold, M.; Zeileis, A.; Scheffer, M. Remotely sensed resilience of tropical forests. *Nat. Clim. Chang.* **2016**, *6*, 1028–1031. [CrossRef]

17. Forzieri, G.; Dakos, V.; McDowell, N.G.; Ramdane, A.; Cescatti, A. Emerging signals of declining forest resilience under climate change. *Nature* **2022**, *608*, 534–539. [CrossRef]

18. Bengtsson, J.; Bullock, J.M.; Egoh, B.; Everson, C.; Everson, T.; O'Connor, T.; O'Farrell, P.J.; Smith, H.G.; Lindborg, R. Grasslands— More important for ecosystem services than you might think. *Ecosphere* **2019**, *10*, e02582. [CrossRef]

19. Boval, M.; Dixon, R.M. The importance of grasslands for animal production and other functions: A review on management and methodological progress in the tropics. *Animal* **2012**, *6*, 748–762. [CrossRef]

20. Bai, Y.; Cotrufo, M.F. Grassland soil carbon sequestration: Current understanding, challenges, and solutions. *Science* **2022**, *377*, 603–608. [CrossRef]

21. Petermann, J.S.; Buzhdygan, O.Y. Grassland biodiversity. *Curr. Biol.* **2021**, *31*, R1195–R1201. [CrossRef] [PubMed]

22. Oliver, T.H.; Heard, M.S.; Isaac, N.J.B.; Roy, D.B.; Procter, D.; Eigenbrod, F.; Freckleton, R.; Hector, A.; Orme, C.D.L.; Petchey, O.L.; et al. Biodiversity and Resilience of Ecosystem Functions. *Trends Ecol. Evol.* **2015**, *30*, 673–684. [CrossRef] [PubMed]

23. Hoover, D.L.; Knapp, A.K.; Smith, M.D. Resistance and resilience of a grassland ecosystem to climate extremes. *Ecology* **2014**, *95*, 2646–2656. [CrossRef]

24. Abdel-Hamid, A.; Dubovyk, O.; Graw, V.; Greve, K. Assessing the impact of drought stress on grasslands using multi-temporal SAR data of Sentinel-1: A case study in Eastern Cape, South Africa. *Eur. J. Remote Sens.* **2020**, *53*, 3–16. [CrossRef]

25. Chen, L.; Sofia, G.; Qiu, J.; Wang, J.; Tarolli, P. Grassland ecosystems resilience to drought: The role of surface water ponds. *Land Degrad. Dev.* **2022**, *34*, 1960–1972. [CrossRef]

26. Yao, Y.; Fu, B.; Liu, Y.; Li, Y.; Wang, S.; Zhan, T.; Wang, Y.; Gao, D. Evaluation of ecosystem resilience to drought based on drought intensity and recovery time. *Agric. For. Meteorol.* **2022**, *314*, 108809. [CrossRef]

27. Tuya, W. Characteristics of grassland utilization in Mongolian Plateauand their differences among countries. *Acta Geogr. Sin.* **2021**, *76*, 1722–1731. [CrossRef]

28. Gao, H.; Huang, Y. Impacts of the Three-North shelter forest program on the main soil nutrients in Northern Shaanxi China: A meta-analysis. *For. Ecol. Manag.* **2020**, *458*, 117808. [CrossRef]

29. Nandintsetseg, B.; Shinoda, M.; Du, C.; Munkhjargal, E. Cold-season disasters on the Eurasian steppes: Climate-driven or man-made. *Sci. Rep.* **2018**, *8*, 14769. [CrossRef]

30. Zhang, Y.; Wang, Q.; Wang, Z.; Yang, Y.; Li, J. Impact of human activities and climate change on the grassland dynamics under different regime policies in the Mongolian Plateau. *Sci. Total Environ.* **2020**, *698*, 134304. [CrossRef]

31. Jamiyansharav, K.; Fernández-Giménez, M.E.; Angerer, J.P.; Yadamsuren, B.; Dash, Z. Plant community change in three Mongolian steppe ecosystems 1994–2013: Applications to state-and-transition models. *Ecosphere* **2018**, *9*, e02145. [CrossRef]

32. Nandintsetseg, B.; Boldgiv, B.; Chang, J.; Ciais, P.; Davaanyam, E.; Batbold, A.; Bat-Oyun, T.; Stenseth, N.C. Risk and vulnerability of Mongolian grasslands under climate change. *Environ. Res. Lett.* **2021**, *16*, 034035. [CrossRef]

33. Nandintsetseg, B.; Shinoda, M. Assessment of drought frequency, duration, and severity and its impact on pasture production in Mongolia. *Nat. Hazards* **2013**, *66*, 995–1008. [CrossRef]

34. Meng, M.; Huang, N.; Wu, M.; Pei, J.; Wang, J.; Niu, Z. Vegetation change in response to climate factors and human activities on the Mongolian Plateau. *PeerJ* **2019**, *7*, e7735. [CrossRef] [PubMed]

35. Liu, X.; Lai, Q.; Yin, S.; Bao, Y.; Qing, S.; Bayarsaikhan, S.; Bu, L.; Mei, L.; Li, Z.; Niu, J.; et al. Exploring grassland ecosystem water use efficiency using indicators of precipitation and soil moisture across the Mongolian Plateau. *Ecol. Indic.* **2022**, *142*, 109207. [CrossRef]

36. Tao, S.; Fang, J.; Zhao, X.; Zhao, S.; Shen, H.; Hu, H.; Tang, Z.; Wang, Z.; Guo, Q. Rapid loss of lakes on the Mongolian Plateau. *Proc. Natl. Acad. Sci. USA* **2015**, *112*, 2281–2286. [CrossRef]

37. Zomer, R.J.; Xu, J.; Trabucco, A. Version 3 of the Global Aridity Index and Potential Evapotranspiration Database. *Sci. Data* **2022**, *9*, 409. [CrossRef]

38. Columbia University. *Gridded Population of the World, Version 4 (GPWv4): Population Density, Revision 11*; NASA Socioeconomic Data and Applications Center (SEDAC): Palisades, NY, USA, 2018.

39. Gilbert, M.; Nicolas, G.; Cinardi, G.; Van Boeckel, T.P.; Vanwambeke, S.O.; Wint, G.R.W.; Robinson, T.P. Global distribution data for cattle, buffaloes, horses, sheep, goats, pigs, chickens and ducks in 2010. *Sci. Data* **2018**, *5*, 180227. [CrossRef] [PubMed]

40. Department of Animal Husbandry. Calculation of reasonable rangeland carrying capacity of natural grassland (NY/T635–2015). Available online: https://www.wdfxw.net/doc43372170.htm (accessed on 12 January 2023).

41. Camps-Valls, G.; Campos-Taberner, M.; Moreno-Martínez, Á.; Walther, S.; Duveiller, G.; Cescatti, A.; Mahecha, M.D.; Muñoz-Marí, J.; García-Haro, F.J.; Guanter, L.; et al. A unified vegetation index for quantifying the terrestrial biosphere. *Sci. Adv.* **2021**, *7*, eabc7447. [CrossRef]

42. Forzieri, G. *MATLAB Codes to Monitor Time-Varying Forest Resilience at Regional-to-Global Scales*; Figshare: London, UK, 2022.

43. Guo, X.; Zhou, H.; Dai, L.; Li, J.; Zhang, F.; Li, Y.; Lin, L.; Li, Q.; Qian, D.; Fan, B.; et al. Restoration of Degraded Grassland Significantly Improves Water Storage in Alpine Grasslands in the Qinghai-Tibet Plateau. *Front. Plant Sci.* **2021**, *12*, 778656. [CrossRef]

44. Lyu, X.; Li, X.; Dang, D.; Dou, H.; Wang, K.; Gong, J.; Wang, H.; Liu, S. A Perspective on the Impact of Grassland Degradation on Ecosystem Services for the Purpose of Sustainable Management. *Remote Sens.* **2022**, *14*, 5120. [CrossRef]

45. Miao, L.; Sun, Z.; Ren, Y.; Schierhorn, F.; Müller, D. Grassland greening on the Mongolian Plateau despite higher grazing intensity. *Land Degrad. Dev.* **2021**, *32*, 792–802. [CrossRef]

46. Gibson, D.J.; Newman, J.A. *Grasslands and Climate Change*; Gibson, D.J., Newman, J.A., Eds.; Cambridge University Press: Cambridge, UK, 2019.

47. Verhoeve, S.L.; Keijzer, T.; Kaitila, R.; Wickama, J.; Sterk, G. Vegetation Resilience under Increasing Drought Conditions in Northern Tanzania. *Remote Sens.* **2021**, *13*, 4592. [CrossRef]

48. Hankerson, B.R.; Schierhorn, F.; Prishchepov, A.V.; Dong, C.; Eisfelder, C.; Müller, D. Modeling the spatial distribution of grazing intensity in Kazakhstan. *PLoS ONE* **2019**, *14*, e0210051. [CrossRef] [PubMed]

49. Bond, W.J.; Stevens, N.; Midgley, G.F.; Lehmann, C.E.R. The Trouble with Trees: Afforestation Plans for Africa. *Trends Ecol. Evol.* **2019**, *34*, 963–965. [CrossRef]